**F. Bourourou[1,*], S. A Tadjer[1], I. Habi[1]**

J. Electrical Systems 07-09 (2022): 166-182

**Regular paper**

# ACTIVE POWER FILTER IMPACT ON POWER QUALITY IMPROVEMENT FOR INDUSTRUAL PLANT SUPPLIED BY PHOTOVOLTAIQUE STATION

Journal of Electrical Systems

This work deals on industrial electrical power quality improvement using an active power filter (APF) based on fuzzy logic controller. The studied system is a PV conversion chain used to supply linear and non-linear industrial loads of 200 kw plant. The PV station is modeled then simulated under Matlab Simulink, with standard conditions consideration in the first time then under real irradiation and sun power variation during the day hours, to obtain the true parameters design of the PV station to be able to give the needed power during the climatic conditions changing. APF parameters design and control loop structure are well studied to have an optimal control. MPPT technique is used in PV station control with the P&O algorithm. Also PV panel fault diagnosis has been done by using alarm for fault indicator and protection over under power. Simulation results are analyzed and discussed comparison with real signals, produced by the FLUK 6001B reference source with the use of the PRS 600 and the Teledyne 3,5 GHz-40Gs/s oscilloscope as measurement instrument, to improve the effectiveness of APF on electrical power quality, THD, amelioration and harmonic minimization in the industrial installation.

Keywords: APF; Faults Diagnostic; FLC; Modelling; PV; power efficiency; Renewable energies

## 1. Introduction

The study presented in this paper is a starting point for an integration of supervising, control and data acquisition (SCADA) system relating to electrical energy quality and active power filters (APF) efficiency, integrated into an industrial area for various administrative companies and industrial production workshops. The main idea is based on PLCs (Programmable Logic Controllers) installed for the control of the APF and the supervision of the quantities affecting the energy quality (Harmonics) of particles (workshops) and all the companies in the industrial zone, This system can be extended, later, to supervise several industrial zones at the same time, figure (1) represent a block diagram of the proposed global system

The idea is inspired from the study presented by Pedro Esteban in May 2020 and which is summarized by the principle diagram of the APF control using a PLC connected to an HMI which is connected by a Ethernet/Modbus TCP/IP bus shown in figure (2) [1] [2] [3].

This configuration type is based on the general principle of remote control and supervision presented in the global diagram block of SCADA communication system shown on figure (3) below [3]:

[*] Corresponding author: Fares Bourourou, Univercity M'Hamed Bougara Boumerdes, Faculty of Hydrocarbure and chimie, Algeria , E-mail: f.bourourou@univ-boumerdes.dz
[1] DJRST, LREEI, Laboratory d'electrification des enterprises industriels, Univercity M'Hamed Bougara Boumerdes, Faculty of Hydrocarbure and chimie, Algeria

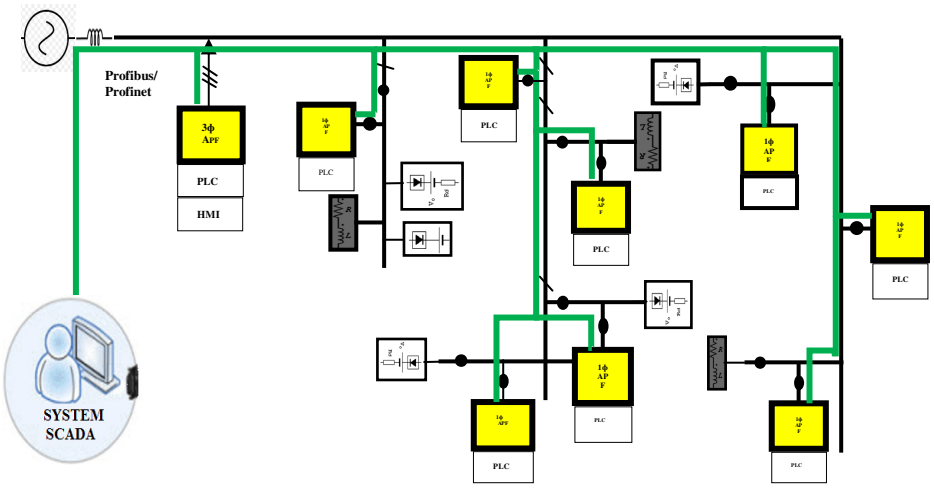


**Figure 1: SCADA configuration for APF control and supervising application**

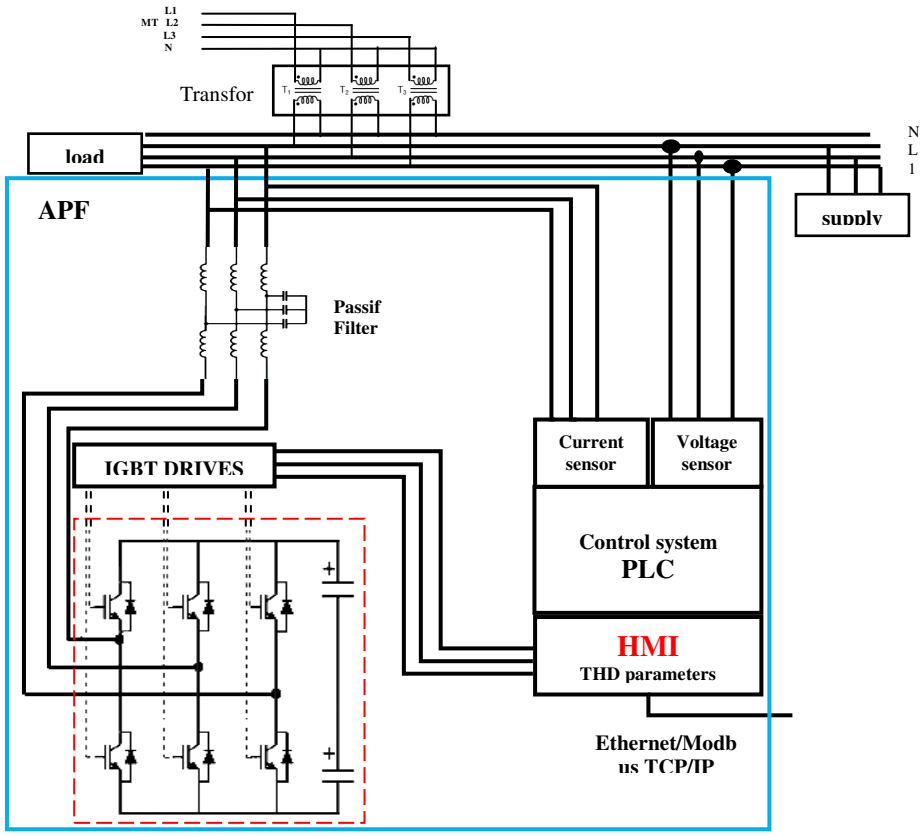


Figure 2: APF controlled by PLC/HMI connected with Ethernet/ Modbus TCP/IP


Figure 3: Schematic diagrams of a SCADA configuration.

## 2. Description of the studied system

When The purpose of this work is to integrate a PV system into the power supply system of an industrial company use power of 200 kw by exploiting the company recorded data, presented in Table (1) with these utilization factors daily, based on the detailed operating principle. Also in order to ensure the quality of the energy produced by the PV system [4] [5-8] dedicated to supplying the company's equipment, an APF will be installed after its sizing with these different control parts and data acquisitions as shown in Figure (4) below[ 9-12] :

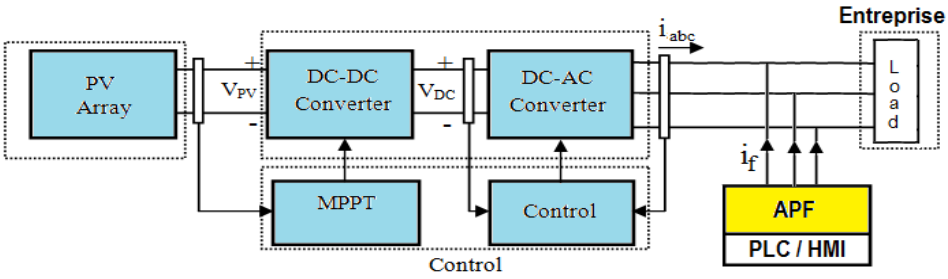


Figure 4: PV system diagrams with APF supplies 200 kw industrial company

The study of each part of the installation leads us to determine the operating system at each hour of the day and the year; the power output in use is a function of the system elements characteristics, data of solar irradiance and temperature.

Modeling of PV system and mainly the solar panels in ideal conditions and simplified after sizing and the deduction of its characteristics make the study of MPPT commands influence on energy quality possible (the output voltage delivered by the proposed PV structure) [5][13].

The required power to supply the plastic articles manufacturing company, which includes electrical machines of different powers, is summarized in the following table (1):

Table 1: Company's various equipment power demands

| Equipment | Power (KW) | Daily usage factor | finally Power (KW) |
|---|---|---|---|
| Asynchronous motor 1 | 34 | 1 | 34 |
| Asynchronous motor 2 | 18.5 | 0.7 | 12.95 |
| Asynchronous motor 3 | 5.5 | 0.7 | 3.85 |
| Asynchronous motor 4 | 1.7 | 0.7 | 1.19 |
| Asynchronous motor 5 | 18.5 | 0.7 | 12.95 |
| Asynchronous motor 6 | 2.4 | 0.9 | 2.16 |
| Asynchronous motor 7 | 2.2 | 1 | 2.2 |
| Asynchronous motor 8 | 4.5 | 1 | 4.5 |
| 9 resistor | 9*1.5 | 0.9 | 12.15 |
| Resistor | 2.5 | 0.9 | 2.25 |
| resistor | 1.5 | 1 | 1.5 |
| Lamps | 12*0.075 | 0.4 | 0.36 |
| Divers | 43 | 0.2 | 8.6 |
| Total | 148.7 | / | 98.66 |

Generally the company start operation at 6h to 8h by elements (11 resistors) which require a power of 15KW, after, a 34KW asynchronous motor will be started, then after 5 min the 2.4KW motor and that of 0.4KW will be started until at 9 a.m or motors of powers 18.5kw, 5.5kw, 1.7kw and 18.5kw and 2.2kw start operation until 1 p.m or motors of

powers 18.5kw, 5.5kw, 1.7kw and 18.5kw and 2.2kw are stopped until 5 p.m then resume its operation another time until 7 p.m, from 7 p.m. until 9 p.m, we are in operation with a power of about 60kw.

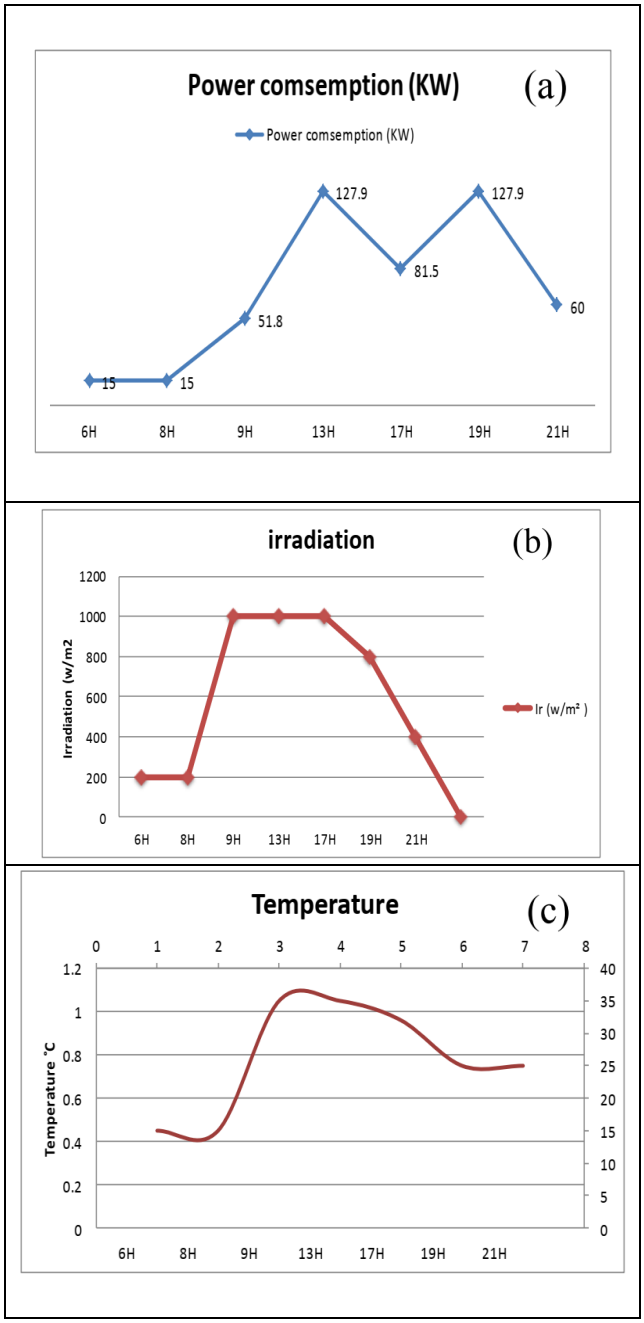


Figure 5: Company machines operating duration (a), Ir (b) and T (c) daily variation Curves

So the PV system must ensure at least the same power necessary for the operation of the company for the same duration, this requires according to the variation of the irradiation and the temperature during the day an equivalent number of panels which must ensure the same power demand, as shown on figure 5 (a), (b),(c)

## 3. PV system plant

### 3.1. PV system parameters Sizing

The PV system parameters sizing requires the study of the main quantities influence on the PV operation ( Ir ; T )

#### 3.1.1 Low illuminance and temperature influence

The efficiency of many commercial modules is not constant and depending on the illumination. This phenomenon is very often neglected by the manufacturers, who give no indication of the behavior of their module at low illumination [13]; the following curves in Figure (6) shows the variation in power values given by a 250 Wp PV panel under standard conditions at a fixed temperature T equal to 25°c variable during the variation in irradiation (a) then T variable with 1000w/m² (b).

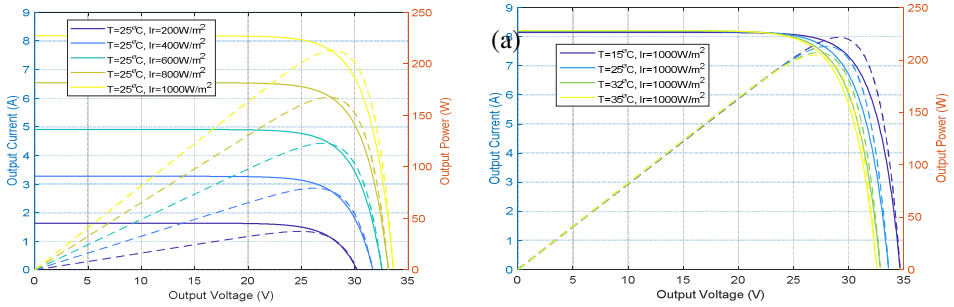


Figure 6: I, P(V) characteristic for different values of irradiance / temperature.

The power delivered by a PV depends on the ambient temperature, the wind speed, the mounting of the module (integrated in the roof or ventilated) and all these parameters change according to the chosen site for modules installation. In addition, the coefficients linked to the temperature differ according to the materials used for the manufacture of the module [13][14].

Temperature is a very important parameter in the behavior of PV cells [15]. Figure (6.b) describes the behavior of the module under a fixed illumination of 1000W/m$^2$, and at temperatures between 15°c and 40°c. We notice that the current increases with the temperature; on the other hand, the open circuit voltage decreases. This leads to a decrease in the maximum power available.

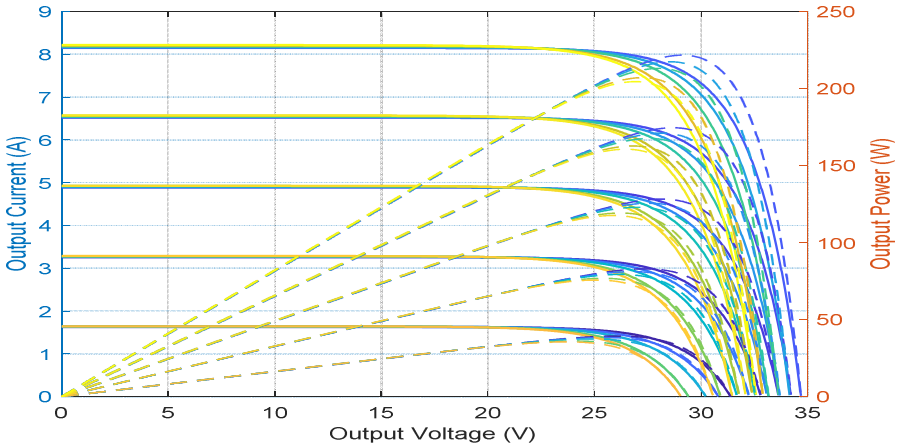


Figure 7: I, P (V) Characteristic for different values of temperature and different values of fixed irradiation.

### 3.1.2. Choice and calculation of panels according to daily consumption

Figure (8) shows the maximum operating point of PV between 6-7h which gives a maximum power of 43W Or the irradiation is about 200 W/m² with temperature 15°c while the machines requiring a power of 15KW (figure 5.a) this makes it possible to calculate the number of panels necessary to ensure such power which is:
15000/43=384 panels which gives 250 W under STC conditions.

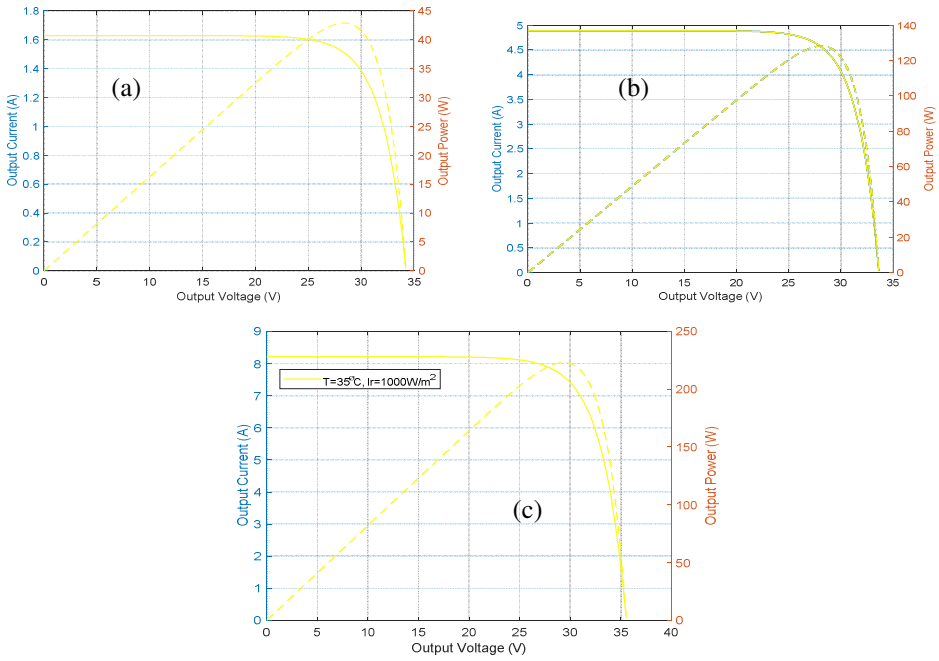

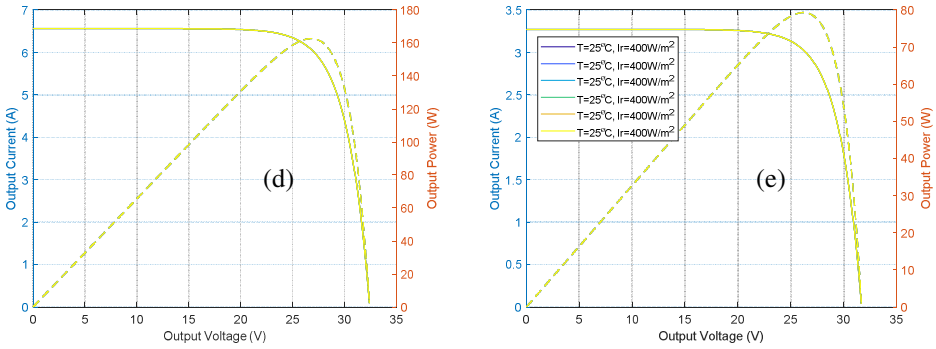


Figure 8: Maximum point PV operating between 6-7am (a), 7-9am (b), 9-5pm (c), 5-7pm (d), 7-9pm 21h(e)

In figure (8.b), between 7-9h which the PV gives a maximum power of 128W or the irradiation is about 600 W/m² with temperature 15°c while the machines requiring a power of 52KW (figure (5.a), So we obtain

52000/128=407 panels which gives 250 W under STC conditions.

In figure (8.c), we obtain 128000/220= 581 panels for 9-13h and 80000/220=364 panels for 13-17h

The curve in figure (9) summarizes the variation of the maximum operating point of the PV (without panels fault) according to the daily variation of temperature and irradiation.

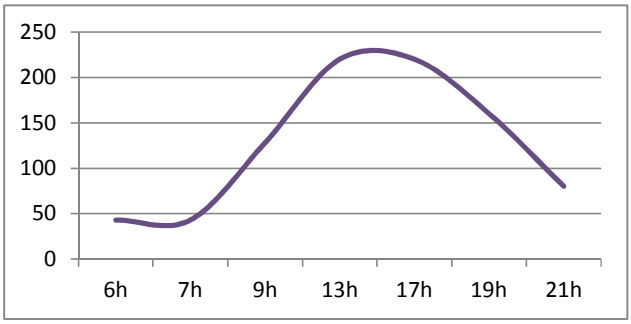


Figure 9: PV Maximum operating point variation

The following table (2) summarizes the general state of the study with consideration of Faults on PV panels

Table 2: power and number of PV corresponding to each period of operation of the company

| day | Temperature °C | Irradiation W/m² | Company power conception KW | Power supplied by the panel (without fault) | Power supplied by the panel (with default) |
|---|---|---|---|---|---|
| 6-7h | 15 | 200 | 15 | 43 | 23 |
| 7-9h | 15 | 600 | 52 | 128 | 70 |
| 9-17h | 35 | 1000 | 9- 13h == 128<br>13-17h == 80 | 220 | 100 |
| 19-19h | 32 | 800 | 128 | 160 | 80 |
| 19- | 25 | 400 | 60 | 80 | 40 |

21h

Table (3) and table (4) summarize the values of power lost due to panels Fault occurs when short circuit in 10 or 20 panel cells happen:

Table 3: Power lost due to the fault on 10 panels: 1.9 % (523 panels)

| Time (heur) | Power (KW) | Power lost due to the fault (W) |
|---|---|---|
| 6-7 | 15 | (43*10-20*10)=230 |
| 7-9 | 52 | (128*10-70*10)=580 |
| 9-13 | 128 | (220*10-100*10)=1200 |
| 13-17 | 80 | (220*10-100*10)=1200 |
| 17-19 | 128 | (160*10-80*10)=800 |
| 19-21 | 60 | (80*10-40*10)=400 |

So if we calculate the power lost on the power supplied by the panel, we obtain the number of panels needed to add to compensate the fault and preserve Company's equipment saves.
For example in the 2$^{end}$ case: 580/128=5 panels added to compensate lost power.

For the further cases, the same number of panels is obtained because of the power supplied by the panel with the presence of a fault, which has decreased in all cases to half the power of the panels without faults.
Solution: PV panel must be added is =5 panels to compensate the lost power.

Table 3: Power lost due to the fault on 20 panels: 3.8 % (523 panels)

| Time (hour) | Power (KW) | Power lost due to the fault (W) |
|---|---|---|
| 6-7 | 15 | (43*20-20*20)=460 |
| 7-9 | 52 | (128*20-70*20)=1160 |
| 9-13 | 128 | (220*20-100*20)=2400 |
| 13-17 | 80 | (220*10-100*10)=2400 |
| 17-19 | 128 | (160*20-80*20)=1600 |
| 19-21 | 60 | (80*20-40*20)=800 |

The study illustrate the influence of the meteorological parameters daily variation, temperature and solar irradiation, on the power produced by the PV system already proposed, sized and modeled, as well as the appearance of a fault at the level of the solar panel. In order to propose, after results analysis, an adequate solution with the diagnosis carried out on the system.

**3.2. PV Diagnosis system Simulation:**

Figure (10) presents the simulation block diagram of an autonomous PV system based on polycrystalline solar panels with a power of 250W under standard temperature and

irradiation conditions (25˚C, 1000W/m²), which supplies a load via a DC-DC-AC converter.

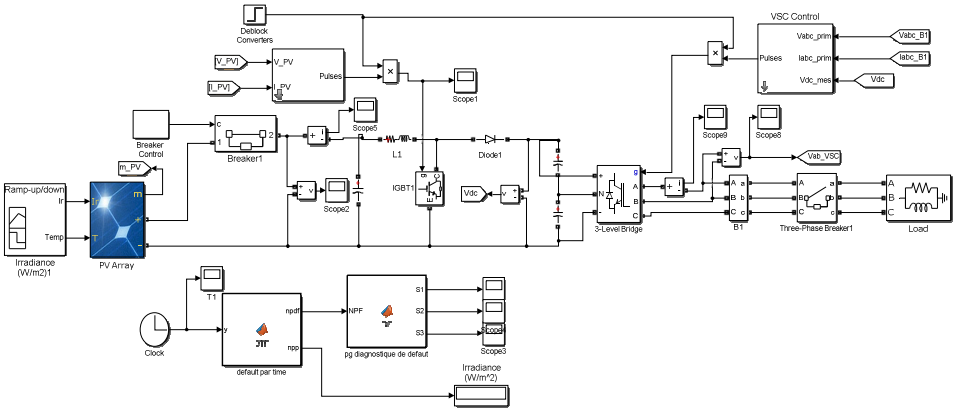


.

Figure 10: PV and Diagnosis system simulation Bloc

Where in Figure (10) presented also the simulation model for fault diagnosis in a PV panel represented by its single diode model and composed from a programming block on Matlab Function for temperature T variation and irradiations G, and another diagnostic block includes the fault and alarm presence indication program or:

- When the PV system has a fault less than 5%, an indication by a pilot lamp (S1) is triggered.
- When the fault becomes more than 5% and less than 10% with the indication of the pilot lamp (S1), an Alarm buzzer (S2) will be activated by the diagnostic program in order to draw attention to the fault increase and the risk of loss of a significant power of that produced by the PV system.
- When the fault exceeds 15% with the lamp (S1) and the buzzer alarm (S2) automatic intervention becomes mandatory in order to protect the equipment, this is ensured by tripping a circuit breaker controlled by the diagnostic program.

There are several topologies of DC-DC converters. They are categorized according to whether the topology is isolated or non-isolated. Isolated topologies employ an isolation transformer operating at high frequency [5] [16], they are very often used in switching power supplies. The most popular topologies in the majority of applications are flyback, half-bridge and full-bridge. In photovoltaic (PV) applications, hybrid systems often employ these types of topologies when electrical isolation is preferred for safety reasons [17]- [23].

### 3. 3. Simulation results Analysis and interpretation:

#### 3.3.1 Case 1 :

Initially, the global system of figure (10) was simulated without the presence of a fault using 250W panels subjected to similar magnitudes of temperature and irradiation.

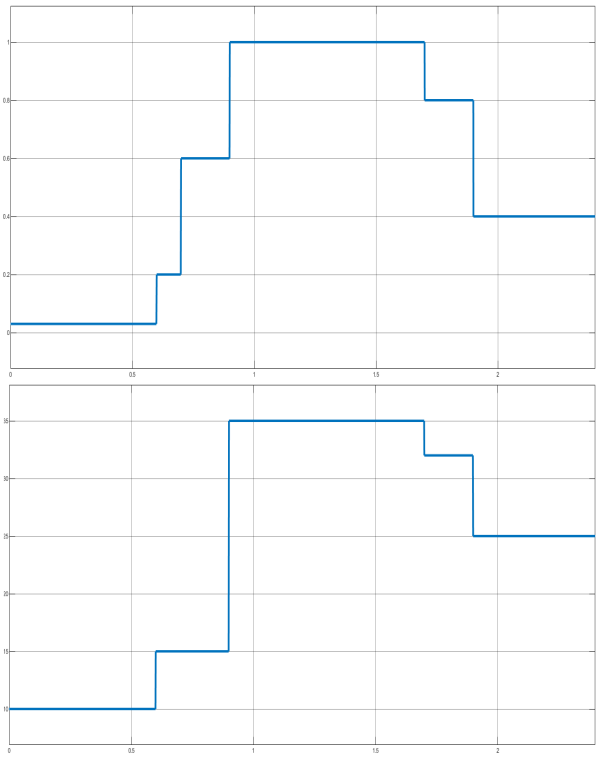

Figure 11: Irradiation and temperature variation curves according to the day hours.

Figure (11) left represents the simulation result on MATLAB/Simulink of an irradiation model (left) where it varies according to the hours of the day from 200W/m² from 6-7h then 600 W/m² from 7-9h and 1000 W/ m² from 9 a.m. to 5p.m. and 800 W/m² from 5 p.m. to 7 p.m. and take a value of 400 W/m² from 7 p.m. to 9 p.m. Where the figure (11) right represents the simulation result on MATLAB/Simulink of a temperature model where it varies according to the hours of the day from 15˚C from 6-7 a.m. then 15˚C from 7-9 a.m. and 15˚C, 35˚C from 9 a.m. to 5 p.m. and 32˚C from 5 p.m. to 7 p.m. and take a value of 25˚C from 7 p.m. to 9 p.m.

This variation in temperature and irradiation allows the PV system to deliver a power corresponding to voltage and current depending on implanted load.

### 3.3.2. Case 2:

In order to follow the influence of the appearance of a fault on the PV panels, we created on the simulation block a set of faults appearing at 7 a.m a fault of 4 defective panels and another fault of 8 panels appearing at 1 p.m and in order to have a precision we have create a greater fault of 16 panels at 15h.

The states S1, S2 and S3 of the fault detection program during the presence of a fault are summarized as follows:

The state of the control signal of the lamp fault presence indicators or note that the lamp is on (S1=0) until the fault is present or the lamp lights up and (S1=1) take the value one. Also note that the alarm is off (S1=0) until the presence of a fault or the alarm is triggered when (S1=1) takes the value one. Also the breaker circuit is closed (S1=0) until the fault presence or the circuit breaker trips when (S1=1) takes the value one.

### 3.3.3. Comparaison

In order to compare the results, the curves of these results are superimposed to visualize the power variation due to the presence of a fault, which is presented in the following figures (12).

It is noticed that the value of the output voltage of the panel during the presence of a fault of 4 defective panels is less than that given before the fault presence, this voltage difference can be visualized better when the fault becomes bigger (8,16 panels).

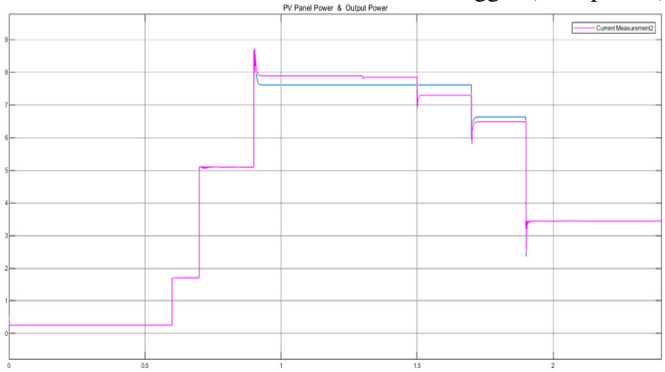


Figure 12: The panel output current during the presence and absence of a fault

It is noted that the value of the power delivered by the panels during the presence of a fault of 4 defective panels is less than that given before the presence of the fault, figure (12), this voltage difference can be visualized better when the fault becomes bigger (8,16 panels) from 230W up to 210W for example.

The alarm program based on the information delivered by the diagnostic and fault detection program which sends a signal comprises the number of panels suffered and has a fault then reacts depending on the case or S1 the control signal of the indicator lamp of fault detection becomes one (1) even when there is a fault of less than 5 faulty panels. In the event that the faults become more than 5 and less than 15 faulty panels with the indicator lamp, a buzzer alarm controlled by S2 is activated. If the fault becomes larger (more serious) with more than 15 faulty panels, a circuit breaker controlled by the S3 signal must be tripped in order to isolate the workshop and ensure the protection of the equipment until the fault is maintained.

### 3.4. Solution

We propose to use a set of panels with power at least able to compensate the lost power when a serious fault appears (more than 15 faulty 250W panels) in order to ensure continuity of service and efficiency energy of the Photovoltaic system and supply the company equipment with the requested power until defective panels repaired.

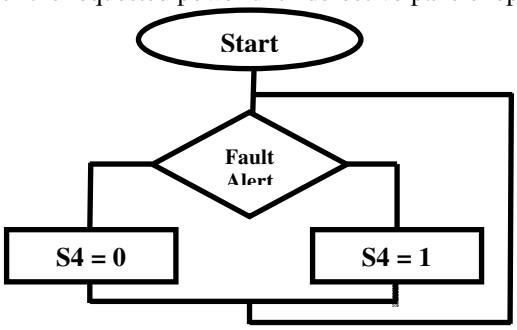


Figure 13: Pv Fault compensation algorithm.

The proposed solution consists of developing an algorithm Figure (13) integrates with the fault diagnosis program and controlling a circuit breaker connecting all the reserve panels to the global PV system then ensuring disconnection when the PV system maintenance is carried out.

## 4. PV Power quality improvement using APF

### 4.1. Proposed structure

Simulation bloc is shown on figure 9 below

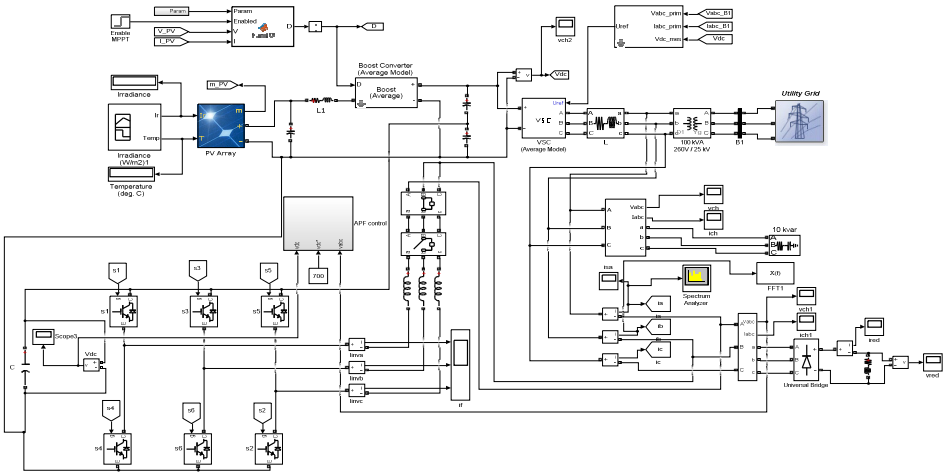


Figure 14: simulation bloc of PV load with APF

The simulation under MATLAB of a photovoltaic structure composed mainly of a set of panels connected in series and in parallel to form a PV field which ensures the supply of an electrical load (company) via a DC-AC converter [10]. The APF is connected to ensure the harmonic detection and the filtering current injection to minimize de THD value of the V and I. For harmonic detection and APF reference compensation currents, many methods can be used, the most several are summarized on figure (15) [19]- [26]

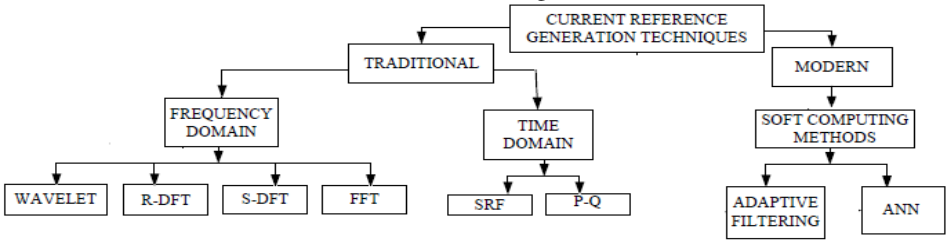


Figure 15: different methodes for APF reference current calculation

The synchronous reference frame method [10] is the best one to have a quickly calculation and the best adapted method with SCADA system because of minimal data needed to have acceptable results, it is based on the transfer of the three phases load current $i_{abc}$ to dq synchronous reference current using park transformation, then the dq components are fed to low pass filter to eliminate harmonic components from fundamental current [11].

The Park invers transformation, is used to convert instantaneous dq component of current into three phase components as shown on figure 11 below

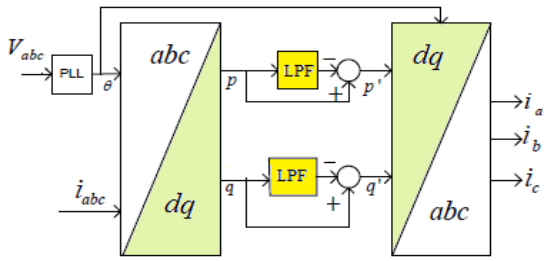


Figure 16: APF reference current calculation by SRF using Park Transformation

### 4.2. APF Control by FLC

APF control loop is based on FLC controller where the membership's function of input and output are represented on figure 17 below:

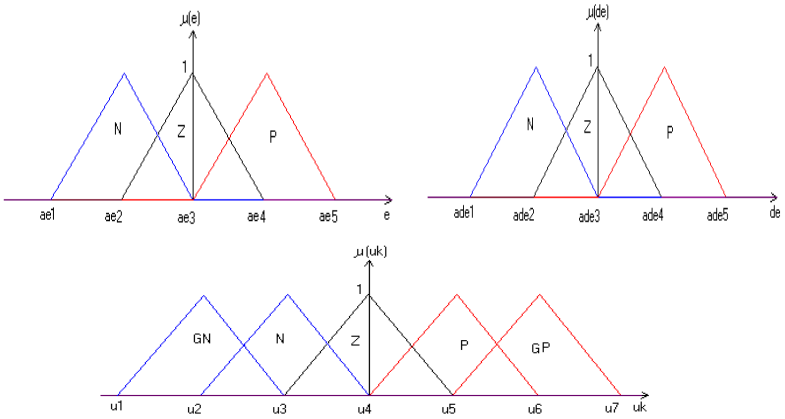


Figure 17: FLC member sheep functions.

Where *e(t )*is the chosen membership functions for error, *de(t)* for error variation and *u(t)* for control output.

The FLC intervals are chosen to have the best fuzzification and defuzzification values.

The controller work based on rules table summarized on table 4:

Table 4: fuzzy logic controller rules

| **Δe/e** | N | Z | P |
|---|---|---|---|
| N | **GN** | **Z** | **Z** |
| Z | **N** | **Z** | **P** |
| P | **Z** | **Z** | **GP** |

Where the table (4) is the result of the use of the logical rules

if ( e<0 & Δe(t)<0) ==> U is GN

if ( e>0 & Δe(t)>0) ==> U is GP

if ( e<0 & Δe(t)>0) or ( e=0 & Δe(t)=0) or ( e=0 & Δe(t)>0) or ( e=0 & Δe(t)<0) or ( e>0 & Δe(t)<0) ====> U is Z.

if ( e<0 & Δe(t)=0) ==> U is N.
if ( e>0 & Δe(t)=0) ==> U is P.

### 4.3. Simulation Results discussion

Simulation results shown that the installation of the APF on the network helps on harmonic minimization as improve the harmonic specter of figure (18).

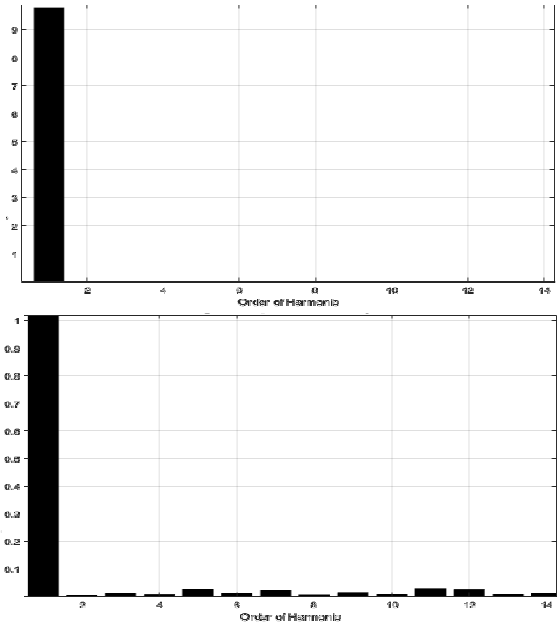

(a) (b)

Figure 18: (a) Harmonic specter with APF use FLC, (b) zoom

This let network current, shown on figure (19), be more near to the sinusoidal wave and the THD value [6,7] decrease from 23,6% to less than 7,46% value.

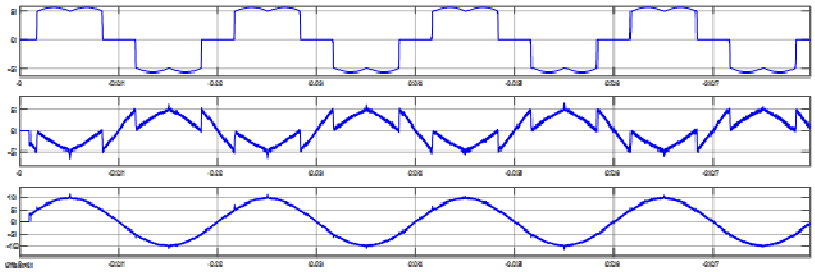

Figure 19: Load, APF and Is currents after APF installation on Network

The APF current is shown on figure (20) below with the load current and PV current after APF connecting.

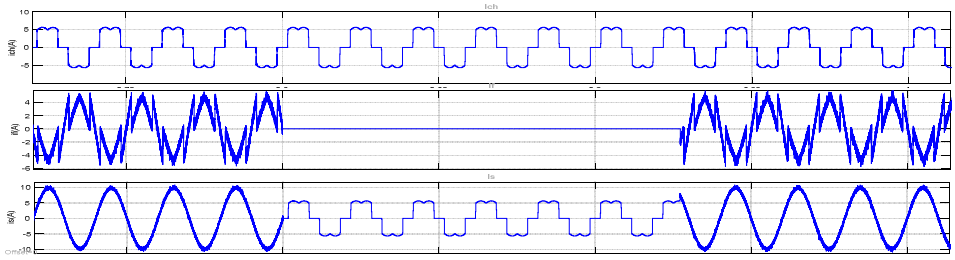

Figure 20: Load, APF & supply delivered Current.

So, APF installation on network has decrease the harmonic presence and this make the PV plant more reliable and regulation system working well as if the THD is more important as it's shown on picture 21 given by the Fluk6100B.

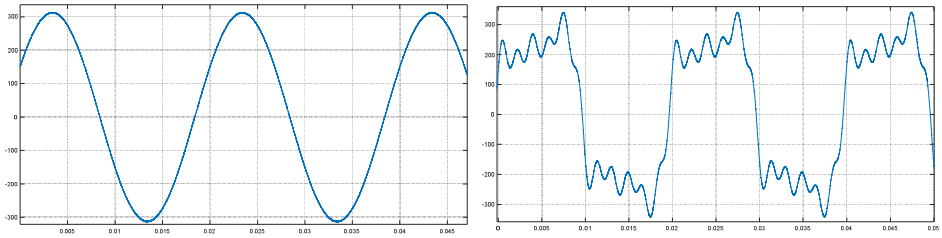

Figure 21: real voltage Measured by the wavepro735Zi-A oscilloscope 4 channels 3,5 GHz with band width 40Gs/s.

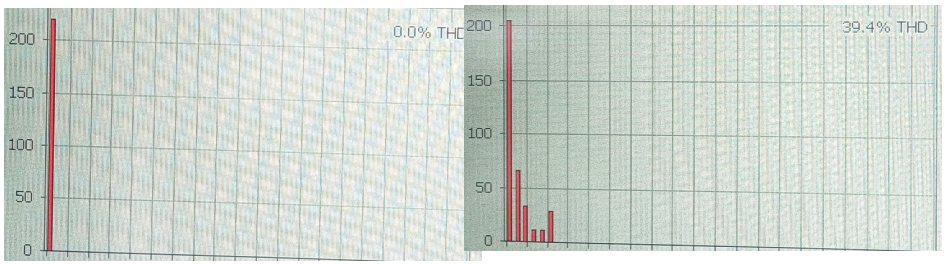


Figure 22: spectre harmonic of a real voltage generated by the fluk 6100B

The Dc voltage of APF capacitor is stabilized by a Fuzzy logic 3x3 controller, as shown on figure (23), where the response time is near to 0.09 second.

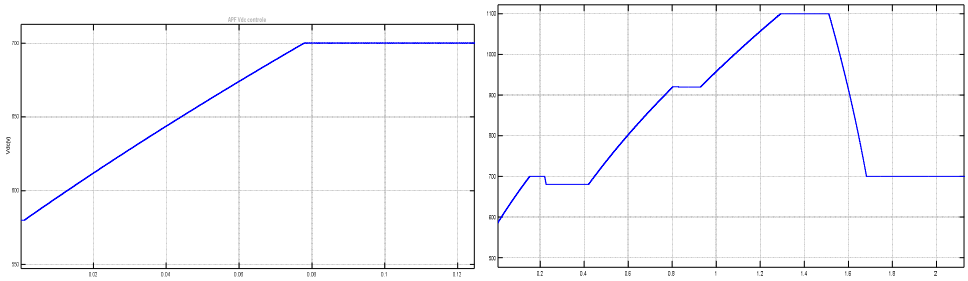

Figure 23: APF Capacitor DC voltage regulation with FLC 3x3 controllers.

The overtaking and response time of APF, $V_{dc}$ voltage regulator, using FLC is 0.09s. Where the 5, 7, 11, 17, 19 and 23 harmonics are reducing to less than 0.03 A from 1.6 A before the use of APF and the THD has decries to less than 7.46%.

## 5. Conclusion

In this work a Simulation under MATLAB of a photovoltaic structure composed mainly of a set of panels connected in series and in parallel to form a PV field which ensures the supply of an electrical load (company) via a DC-DC-AC converter Controlled in MPPT based on the P&O technique during the presence of certain faults of varying degree monitored by a diagnostic system based on a fault detection algorithm. The obtained results analysis confirm the efficiency of the proposed diagnostic system and the compensation of the power lost during fault appearance, which ensures energy efficiency of the photovoltaic system in the company's power supply.

The PV power sizing is based on statistic studies of sun power and temperature variation during climatic changing over the day, Faults can be appeared on PV panel is Also resolved by the proposition of a Diagnostic algorithm connected to indicator lamp when fault is les then 5 Panel and a sound Alarm with the lamp if the fault greater than 5 panel but when fault gone bigger a fault controlled breaker trigger to isolate the plant from PV station and protect equipment from the under voltage and power messing.

The PV plant connected to the network via a rectifier connected to an inverter supply linear and nonlinear loads of 200kw industrial plant voltage and currents are analyzed using the FFT method for power quality supervise and control; results are compared with the reference signals generated by the FLUK 6001B reference source with the use of the PRS 600 and the wavepro735Zi-A oscilloscope, 4 channels 3.5 GHz with band width 40 Gs/s, as measurement instrument Harmonic due to the presence of Nonlinear loads has been decrease by the use of a three phase shunt APF controlled by an FLC 3x3 rules. The APF installation on the network has decrease the THD of the network current from 23.6% to less than 7.46%.

Finely we hope applied more intelligent techniques to the studied system with hybrid electrical power of renewable energy to have more suitable results for industrial factory and achieve the power efficacy of renewable energy plants.

**Acknowledgment**

Our best gratefully acknowledge are sent to the LREEI Laboratory Director, Faculty of Hydrocarbons and chemistry in the university M'hamed Bougara of Boumerdes, Algeria.

**References**

[1] Khechiba kamel, et al., Comparison of Control Strategies for Shunt Active Power Filters in Three-Phase Three-Wire Systems, The 3rd International Conference on Power Electronics and their Applications ICPEA 2017, Djelfa, Algeria, 16-17, 2017.

[2] Vodapalli Prakash,T.RamaSubbaRed dy, S.TaraKalyani,P.B.Karandikar, integration of photovoltac energy for improving power quality of UPQC, J. Electrical Systems 17-1, p 105-120,2021.

[3] S. Masoum et al., Microprocessor-controlled new class of optimal battery chargers for photovoltaic application, Vol. 19, September, 2004

[4] Tarek Bouktir, Linda Slimani, B Mahdad, Optimal power dispatch for large scale power system using stochastic search algorithms, International Journal of Power and Energy Systems, Vol. 28, No. 2, 2008.

[5] Petit, F. J. Robles, Guillermo. Amarís, Hortensia, Current Reference Control for Shunt Active Power Filters under Nonsinusoidal Voltage Conditions, IEEE Transactions on Power Delivery, vol. 22, no. 4, 2254-2261, 2007.

[6] Linda Slimani, Tarek Bouktir, Optimal power flow solution of the Algerian electrical network using differential evolution algorithm, Revue Telkomnika, 2012.

[7] Belhaouchet nouri, Fonctionnement à Fréquence de Commutation Constante des Convertisseurs de Puissance en Utilisant des Techniques de Commande Avancées Application : Amélioration de la Qualité de l'Energie, Thèse Doctorat en sciences, Electrotechnique, Université FERHAT ABBAS – SETIF, 2011.
[8] Long Bun, Détection et Localisation de Défauts pour un Système PV; thèse de doctorat ; L'université de Grenoble, 2011
[9] Nopporn Patcharaprakiti, Maximum power point tracking using adaptive fuzzy logic control for grid-connected photovoltaic system, Renewable Energy 30, 2005.
[10] Tadjer Sid Ahmeda, et al., Direct components extraction of voltage in photovoltaic active filter connected in a perturbed electrical network (based on robust PLL algorithm), International Conference on Technologies and Materials for Renewable Energy, Environment and Sustainability, TMREES15; science direct Energy Procedia74 (2015) 966 – 972, 2015.
[11] P. Mattavelli, synchronous frame harmonic control for high performance AC power supplies, IEEE Trans. Ind. Applicat, Vol 37,No 3, pp.864-872, 2001.
[12] L.L.M and S. Sunandha, mitigation of harmonics by fuzzy logic control based active filter with different fuzzy membership functions, Journal of Chem. Pharm. Sci., No. 8, pp. 133-138, 2016.
[13] Ghadbane Ismail, "Etude Et Réalisation D'un Filtre Actif Parallèle En Utilisant Différentes Stratégies De Contrôle", Thèse Doctorat en sciences, Electrotechnique, Université Mohamed Khider – Biskra, 2016.
[14] L. Zelloumaa,, et al.;Fuzzy logic controller of five levels active power filter, Energy Procedia 74 ( 2015 ) 1015 – 1025, elsevier 2015.
[15] V. Salas, E. Olias, A. Barrado, A. Lazaro, Review of the maximum power point tracking algorithms for standalone photovoltaic systems , Solar Energy Materials & Solar Cells 90, 2006.
[16] B. Boukezata, A. Chaoui, J.P. Gaubert, and M. Hachemi, Photovoltaic solar system connected to the electrical network and associated with a parallel active filter, Electrical Engineering Symposium, Cachan, 2014.
[17] V. Boitier, P. Maussion, C. CABAL, Recherche du maximum de puissance sur les générateurs photovoltaïques, Université de Toulouse, 2008.
[18] O. Boukli-Hacene, Conception et réalisation d'un générateur photovoltaique muni d'un convertisseur MPPT pour une meilleure gestion énergétique, These de Magister Univercité Tlemcen, 2011.
[19] Mahamat Defallah DJAMALADINE, Etude et conception d'une chaine photovoltaïque connectée au réseau et étude de la qualité de l'énergie injectée, Université de Tunis - Mastère II Recherche 2016.
[20] Mishra, D. P., & Ray, P. Fault detection, location and classification of a transmission line. Neural Computing and Applications, 30 5, 1377-1424, 2017.
[21] Marcolino Humberto Díaz-Araujo, Aurelio Medina-Rios, Manuel Madrigal-Martínez and Luis Arthur Cleary-Balderas, Analysis of Grid-Connected Photovoltaic Generation Systems in the Harmonic Domain, Energies 12. 2019.
[22] Amal A.Hassan, Faten H. Fahmy, Abd El-Shafy A.Nafeh, Hosam K. M. Youssef ,Control of Three-Phase Inverters for Smart Grid Integration of Photovoltaic Systems, J. Electrical Systems 18-1, p 109-131, 2022
[23] Laid zellouma, et al.,simulation and real time implementation of three phase four wire shunt active power filter based on sliding mode controller, Rev. Roum. Sci. Techn.– Électrotechn. et Énerg, Vol. 63, 1, pp. 77–82, Bucarest, 2018.
[24] M.T. Benchouia, et al., Implementation of adaptive fuzzy logic and PI controllers to regulate the DC bus voltage of shunt active power filter, Applied Soft Computing, 28, pp. 125–131, 2015.
[25] G. Gantaiah, Swamy1, Padma Kottala, Wavelet-ANN Based Analysis of PV IoT Integrated Two Area Power System Network Protection in presence of SVC, J. Electrical Systems 18-1 , p 23-38, 2022
[26] O. Boukli-Hacene, Conception et réalisation d'un générateur photovoltaique muni d'un convertisseur MPPT pour une meilleure gestion énergétique, These de Magister Univercité Tlemcen, 2011.